Available online at www.sciencedirect.com
ScienceDirect
Russian Geology and Geophysics 50 (2009) 136–142
RUSSIAN GEOLOGY AND GEOPHYSICS
www.elsevier.com/locate/rgg

Joint inversion of IP-affected TEM data

N.O. Kozhevnikov *, E.Yu. Antonov

Trofimuk Institute of Petroleum Geology and Geophysics, Siberian Branch of the RAS, 3 prosp. Akad. Koptyuga, Novosibirsk, 630090, Russia

Received 28 December 2007; accepted 16 June 2008

Abstract

A numerical experiment was applied to explore the potentialities and limitations of joint inversion of IP-affected transients measured with different loop configurations above a uniform half-space with a Cole-Cole complex conductivity. One of us calculated 200 m × 50 m and 50 m × 50 m loop responses of a uniform polarizable conductor with varied Cole-Cole parameters and imposed synthetic Gaussian noise that simulated measurement errors. Then the generated pseudo-experimental data passed to the other co-author who performed single and joint 1D inversion twice: first being unaware of the "true" underlying models and then after being told that they all were represented by a uniform polarizable earth. More than a half of the fitted models provided a good idea of the true models though misfit was quite large in some cases. The fit was better in single inversion with a priori information available, and improved further through joint inversion of central-loop and coincident-loop responses. Joint inversion with a priori information known was of good quality even at a chargeability as low as 0.02. The standard error in joint inversion was times the measurement error and depended mainly on fitting errors for smaller-loop data. The reason is that the smaller-loop transients included a non-monotonous interval where the signal changed rapidly under the effect of fast-decaying induced polarization.

Keywords: Induced polarization; TEM method; single and joint inversion; frozen ground

Introduction

In our previous paper (Kozhevnikov and Antonov, 2007) we discussed a numerical experiment in which we investigated the potentialities and limitations of single inversion of 100 m × 100 m coincident loop responses of a uniform conductive and polarizable earth. The inversion was performed twice: first the interpreter was unaware of the "true" reference models and then repeated the procedure with a priori knowledge. At a low chargeability the quality of inversion in the former case was quite low for some models, and the responses were explainable in terms of a nonpolarizable layered earth. However, more than a half of the fitted models provided a good idea of the starting models. The Cole-Cole parameters found by inversion of the pseudo-experimental data with the starting models known to be of a 10^3 ohm·m uniform polarizable earth approached those in the true models even at low chargeability (η) and exponent (c).

Kamenetsky et al. (1990) showed, within the limits of a preliminary theory of fast-decaying IP effect on the transient process, that the normally induced vortex currents and the polarization currents had different patterns depending on loop configuration. Therefore, it appeared possible to amplify or damp IP effects by changing loop configuration and to discriminate the inductive and polarization components by using loops of different sizes at the same site.

Note that this discrimination is possible — as a certain approximation — only if polarizability is low or if IP and normally induced vortex current decay at different characteristic times (Sidorov and Yakhin, 1979). The only general way of inversion of TEM data from a conductive polarizable earth is to use forward models that account for frequency dependence of conductivity and/or dielectric permittivity of rocks.

With today's computing facilities and fast algorithms, it is possible to compare directly single and joint inversion of coincident- and central-loop transients, including IP-affected responses, to estimate the performance of different methods. It is this feasibility, together with the shortage of literature on joint inversion of IP-affected TEM data, that motivated the reported numerical experiment.

Methods

The numerical experiment was designed in a way to provide the most faithful simulation of the reality. One of us

* Corresponding author.
E-mail address: KozhevnikovNO@ipgg.nsc.ru (N.O. Kozhevnikov)

1068-7971/$ - see front matter
doi:10.1016/j.rgg.2008.06.021

(N. Kozhevnikov) selected initial models, computed synthetic transients, and imposed synthetic random noise; the other (E. Antonov) inverted the generated pseudo-experimental responses in terms of a layered polarizable, conductive earth. The experiment consisted of two steps. We chose a reference model of a uniform conductive and polarizable earth with Cole-Cole parameters common to real ion-conductive frozen ground for several reasons detailed in (Kozhevnikov and Antonov, 2007).

Fast-decaying IP was included through the complex frequency-dependent conductivity $\sigma*(\omega)$, according to the Cole-Cole model

$$\sigma^*(\omega) = \sigma_0 \frac{1 + (j\omega\tau)^c}{1 + (1 - \eta)\,(j\omega\tau)^c},$$

where $j = \sqrt{-1}$; ω is the angular frequency, in s^{-1}; σ_0 is the dc conductivity, in S/m; η is the chargeability ($0 \le \eta \le 1$); c is the exponent ($0 \le c \le 1$)); τ is the relaxation time, in s (Lee, 1981; Svetov et al., 1996).

The synthetic IP-affected TEM responses were computed using software specially designed by E. Antonov.

The inversion of computed synthetic transients was run twice, without and with a priori information: First E. Antonov was unaware of the true reference models and then he repeated the procedure after being told that they all were of a uniform polarizing earth.

To estimate the effect of fast-decaying IP on the transients, we used five models of a uniform polarizable half-space with $\rho = 100$–2000 ohm·m, $\eta = 0.02$–0.5, $\tau = 10^{-5}$–$2{\cdot}10^{-4}$ s, c = 0.4–1.0; such parameters are characteristic of ion-conductive frozen ground. The choice of parameters was made random in order to avoid biases toward a "good" set (at which the success of inversion would be more certain). See the list of thus generated models in Table 1.

With each of the five models, the transients were computed for a central-loop (200 m × 200 m transmitter and 50 m × 50 m receiver) and a 50 m × 50 m coincident-loop configurations. The 200 m × 50 m size of the former was chosen according to the usual practice of TEM soundings. The choice of the smaller coincident loop was made for two reasons. First, the transients measured by the two systems at different sites were expected to bear clearly different contributions from IP and normally induced vortex currents because of the four-fold difference in electrode spacing, which was a good prerequisite for joint data inversion (Kamenetsky et al., 1990). Second, such configuration would be handy in the field as it is easy to lay another 50 m × 50 m loop once a central receiver loop has been already set up.

Table 1
Models of polarizable half-space used to estimate quality of joint inversion

Model	ρ, ohm·m	η	τ, s	c
1	100	0.1	$5{\cdot}10^{-5}$	0.6
2	200	0.02	$1{\cdot}10^{-4}$	0.7
3	500	0.2	$2{\cdot}10^{-4}$	0.4
4	1000	0.05	$1{\cdot}10^{-5}$	0.9
5	2000	0.5	$2{\cdot}10^{-5}$	1

Field measured transients commonly bear external random noise and instrumental errors. Mind that measuring instruments in the TEM method are normally designed with an effective bandwidth decreasing from early to late times. Thus, although the responses decay, the electromagnetic noise likewise decreases progressively leaving the signal-to-noise ratio almost invariable in a broad time range, whence noise ≅ const × signal. This very noise, called multiplicative noise, was added to synthetic transients by generation of a Gaussian series of random numbers. The random-number sequence which simulated multiplicative noise had a mean of $\mu_n = 1$, and a relative standard error associated with random noise was assumed according to the level expected for a given configuration. The emf of synthetic transients were multiplied by a random number from the sequence at each time delay, to eventually obtain a rms error of σ_n in all data making up a transient.

The use of a larger transmitter loop was expected to provide a greater moment than with a smaller loop. Therefore, we assumed that the standard errors from the added multiplicative noise were $\sigma_n = 0.02$ for the central loop and $\sigma_n = 0.05$ for the coincident loop.

The imposed Gaussian noise corresponding to ADC quantization and other instrumental errors depended on receivers but was independent of loop configuration, with a zero dc component and $\sigma_n = 0.1$ μV.

The time range of the generated transients was defined by the transmitter loop size and instrumental facilities. The delay times started at 10–30 μs because, according to the field experience, the transient self-responses in the measurement systems decay at 10 μs and 30 μs for 50 m × 50 m and 200 m × 50 m loops, respectively (Vanchugov and Kozhevnikov, 1998). The latest delay time was 100 ms for all synthetic responses; the times used in inversion varied depending on different resistivity models but extended to no more than 1.3 ms for the 50 m × 50 m loop and 6 ms for the 200 m × 50 m loop. These values corresponded to the limit where the responses were less than 0.1 μV in order of magnitude.

Figure 1 shows pseudo-experimental transients and those fitted through joint inversion for models 3 and 5 (Table 1). In the case of Fig. 1, *a*, the smaller-loop response unambiguously indicates the presence of fast-decaying IP (monotony break and sign reversal at 260 μs), while that of the large loop looks in quite a normal way, i.e., it remains positive and no IP effect appears. This response can be formally interpreted in terms of a nonpolarizable layered earth (Kozhevnikov and Antonov, 2007).

Both transients in Fig. 1, *b* show sign reversal: at 105 μs for the 50 m × 50 m loop and at 90 μs for the 200 m × 50 m loop. Note that this is the second sign reversal followed by positive emf. The relaxation time τ for model 5 being as short as 20 μs, the first sign reversal is too early to be detected with the 50 m × 50 m loop, and more so, with the large loop.

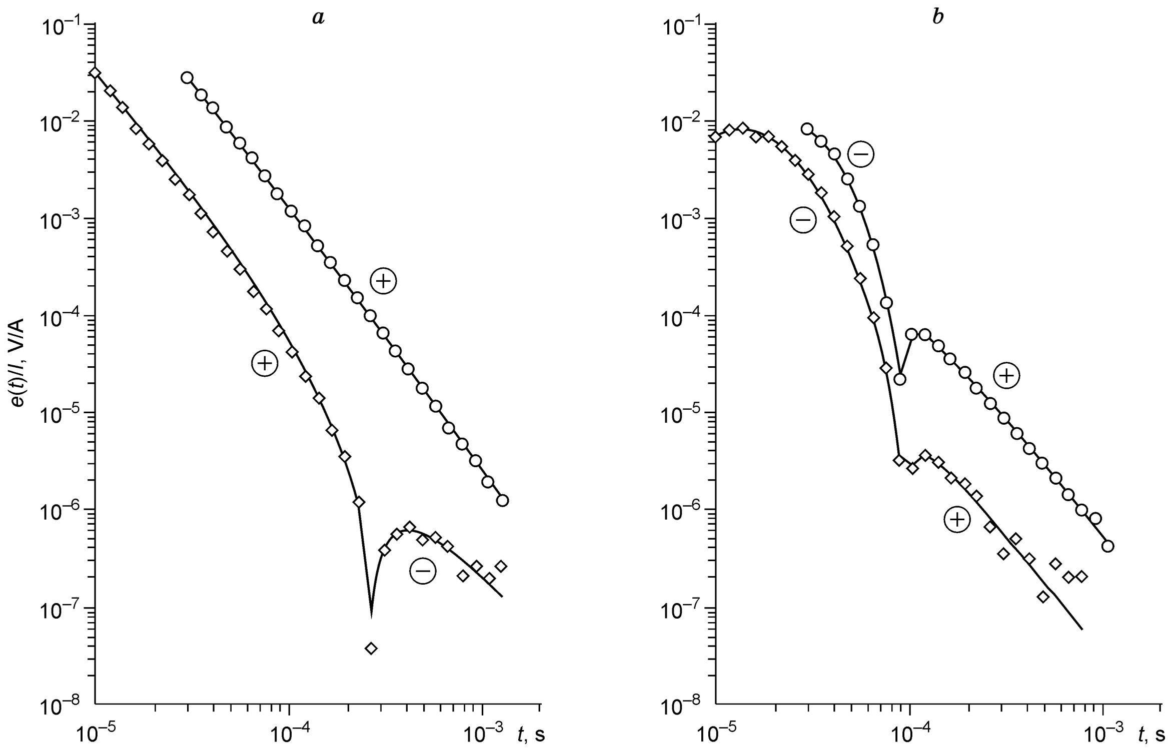

Fig. 1. Coincident-loop (diamonds) and central-loop (open circles) pseudo-experimental and fitted (solid line) transients: *a* — model 3, *b* — model 5 (Table 1). Circled plus and minus mark, correspondingly, positive and negative parts of responses.

The inverse problem was solved by fitting a set of parameters from the space of model data to provide the minimum of the objective function $\varphi(\mathbf{P})$:

$$\varphi(\mathbf{P}) = \left\{ \frac{1}{N-1} \sum_{i=1}^{N} \left[\frac{\varepsilon^{\text{expr}}(t_i) - F_{\mathbf{P}}(t_i)}{\delta(t_i)\varepsilon^{\text{expr}}(t_i)} \right]^2 \right\}^{1/2}, \qquad (1)$$

where t_i is the i-th time delay, N is the total number of time delays; $F_{\mathbf{P}}$ is the forward operator; $\delta(t_i)$ is the relative measurement error at the delay t_i. The objective function is the weighted mean sum of squares of relative differences between the fitted and pseudo-experimental transient responses. The set of model parameters is the vector $\mathbf{P} = (\sigma_j, h_j, \eta_j, \tau_j, c_j)|_{j\,=\,1,\,M}$, where M is the total number of layers, σ_j is the conductivity, h_j is the layer thickness, η_j is the chargeability, τ_j is the IP relaxation time constant, and c_j is the exponent for the j-th layer.

The problem was solved using a modified algorithm by Nelder and Mead (1965), which is one of the best forward tools for minimization of multivariable functions that require no derivatives of forward functions to be included into the equation of minimized functional.

The joint inversion of transients differed from the single inversion in that the objective function included data for both loops, i.e., $N = N_1 + N_2$, where N_1 is the number of delays and data for the first loop and N_2 is that for the second loop. Unlike the single inversion of 100 m × 100 m coincident-loop data (Kozhevnikov and Antonov, 2007), the synthetic transients of the two loops were calculated using forward runs with regard to the loop configuration. To put it different, the total forward operator $F_{\mathbf{P}}$ comprised the operators $F_{\mathbf{P}_1}$ and $F_{\mathbf{P}_2}$: the former used for 200 m × 50 m central-loop transients and the latter for the 50 m × 50 m coincident-loop responses. The measurement errors $\delta(t_i)$ included in (1) were different in the two systems, and the errors were thus assumed to be 2% at $1 \le i \le N_1$ and 5% at $N_1 + 1 \le i \le N$.

It is pertinent to mention the relative contributions of transients from both loops into the joint goal function. As we wrote above, the 200 m × 50 m loop transients extended to later times than those of the 50 m × 50 m loop. On the other hand, the latter can resolve signals at earlier times than the former. So, the difference was not so great though the number of counts N_1 for the 200 m × 50 m loop was usually greater than N_2 for the 50 m × 50 m loop. Therefore, the statistic weight of transients was defined mainly by the $\delta(t_i)$ error included in the objective function.

Results and discussion

At the first step of the experiment, the generated transients were inverted without any knowledge of the reference models, but the form of the responses caused the interpreter to guess a two-layer earth model. Inversion began with the 50 m × 50 m coincident-loop responses, then fitting was applied to the central-loop data, and, finally, both data sets were inverted jointly.

Table 2
Results of inversion without a priori information

Parameter	Model 1			Model 2			Model 3			Model 4			Model 5		
	1	2	3	1	2	3	1	2	3	1	2	3	1	2	3
H_1, m	18	4.3	0.1	4.1	0.7	0.13	7.8	4.8	0.44	97	230	228	2.3	11.8	160
ρ_1, ohm·m	82	62	42	174	290	185	240	202	217	1004	990	992	970	999	1390
η_1	0	0	0	0	0	0	0	0	0	0.047	0.049	0.053	0.7	0.67	0.45
τ_1, μs	—	—	—	—	—	—	—	—	—	10	13	10.4	38	38	17
c_1	—	—	—	—	—	—	—	—	—	0.92	0.94	0.91	0.99	0.95	0.98
ρ_2, ohm·m	135	106	100	204	201	200	540	537	494	1040	1040	1040	2000	1960	3000
η_2	0.03	0.07	0.12	0.05	0.03	0.08	0.14	0.13	0.15	0.05	0.04	0.04	0	0	0
τ_2, μs	23	19	38	14	5.6	1.2	3.1	400	190	1	0.3	0.69	—	—	—
c_2	0.44	0.41	0.55	0.42	0.39	0.35	0.54	0.54	0.53	0.84	0.89	0.91	—	—	—
σ, %	6.1	4	7.1	5	3	6.4	24	2.4	18.4	4.7	3.2	5.7	30	9	42

Note. 1, 2 — single inversion of coincident-loop (1) and central-loop (2) transients and 3 — their joint inversion, here and in Table 3.

First three recovered models (Table 2) included a polarizable layer under a nonpolarizable overburden, both layers were polarizable in the fourth model, and the fifth model corresponded to a polarizable layer above a nonpolarizable basement. Relative standard error was in a range of 2.5 to 42% and did not exceed 10% for eleven of fifteen models (Table 2).

Once inversion without a priori information had been completed, the interpreter learned that all models were represented by a uniform polarizable half-space and repeated the procedure. See the respective columns of Table 3 for the resulting model parameters and standard errors.

According to the succession of steps in the experiment, we discuss first the results of inversion without a priori knowledge. As in the case of single inversion of 100 × 100 m coincident-loop data (Kozhevnikov and Antonov, 2007), the results may seem discouraging because the inversion procedure drove to a two-layer model with one or two polarizable layers instead of a uniform half-space. However, things turn better if one looks at the layer thicknesses in the five models (Fig. 2, *a*). In models 1, 2, 3 with a nonpolarizable layer above and a polarizable base below, the upper layer had a thickness (H_1) smaller than the loop characteristic size r and its effect was thus minor. Therefore, the two-layer earth could be approximated by a uniform polarizable half-space with the parameters of the lower layer. That is, inversion for models 1, 2, 3 actually gave a nearly uniform polarizable half-space with $\rho = \rho_2$, $\eta = \eta_2$, $\tau = \tau_2$, $c = c_2$ (Fig. 3).

Model 4 was found to be a two-layer earth with a polarizable layer (ρ_1, η_1, τ_1, c_1) over a base with (ρ_2, η_2, τ_2, c_2). The thickness of the upper layer H_1 = 100 to 230 m exceeded the characteristic sizes of both loops (200 m × 50 m and, more so, 50 m × 50 m). The IP time constant τ_2 being < 1 μs, one may assume that $\eta_2 = 0$ within the common TEM time range. Therefore, the model likewise approached a uniform polarizable half-space with $\rho = \rho_1$, $\eta = \eta_1$, $\tau = \tau_1$, $c = c_1$.

Finally, model 5 was a polarizable layer with ρ_1, η_1, τ_1, c_1 over a nonpolarizable base with the resistivity ρ_2. Single inversion of transients for the two loops gave a bad result as the upper layer was thin. However, joint inversion resulted in a thickness of 160 m to allow again a uniform half-space approximation with $\rho = \rho_1$, $\eta = \eta_1$, $\tau = \tau_1$, $c = c_1$ (Fig. 3).

See normalized inversion-derived parameters in Fig. 2, *b–f*. Note that imaging inversion data in an elegant easily readable way may be a problem. To help this, one can assume some Cole-Cole parameter (say, chargeability, η) to be independent and plot it against normalized values of the respective fitted parameter (Kozhevnikov and Antonov, 2007). In Fig. 2, *b–f* and in Fig. 4 (see below), η, τ, and c are the "true" parameters

Table 3
Results of inversion with a priori information

Parameter	Model 1			Model 2			Model 3			Model 4			Model 5		
	1	2	3	1	2	3	1	2	3	1	2	3	1	2	3
ρ, ohm·m	91	100	100	200	202	200	515	495	494	1040	1030	1000	1990	2000	2000
η	0.75	0.83	0.14	0.04	0.033	0.016	0.14	0.14	0.14	0.037	0.002	0.05	0.5	0.5	0.5
τ, μs	0.6	0.2	26	20	0.3	130	210	290	200	11	0.4	10.5	20	20	20
c	0.42	0.42	0.48	0.4	0.24	0.7	0.54	0.53	0.54	0.96	0.99	0.9	1	1	1
σ, %	6.4	4	7.1	5.5	3.3	5.7	26	2.5	22.6	5	4.3	6	25	5.4	21

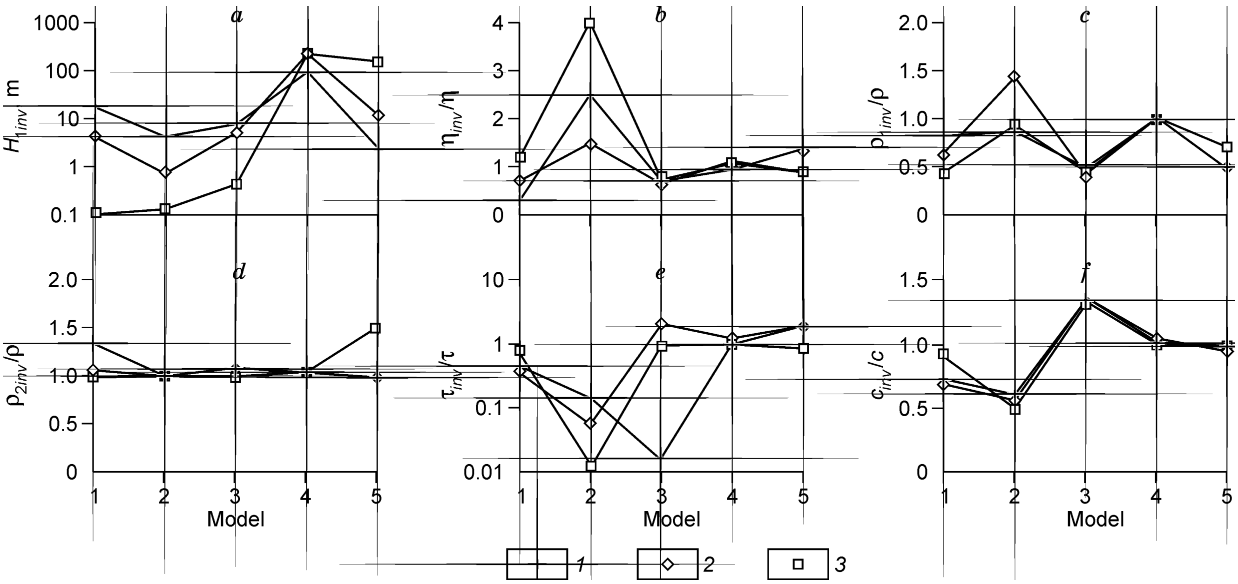

Fig. 2. Parameters obtained by single inversion of coincident-loop (*1*) and central-loop (*2*) transients and their joint inversion (*3*), for different models (Table 1); inversions were done in the absence of a priori information. *a–e* are explained in text.

(i.e., those assumed in computing pseudo-experimental transients) and η_{inv}, τ_{inv}, and c_{inv} are the fitted ones. The η_{inv}/η, τ_{inv}/η, and c_{inv}/c ratios represent relative deviations of the fitted parameters from the true values. The plots in Fig. 2, *b*, *e*, *f* were obtained using the chargeability, the time constant, and the exponent from the layers interpreted as a uniform earth (Fig. 3).

Resistivity needs a special comment. Although a two-layer fit could be justified, resistivities in both layers were about the resistivity in the true uniform-earth model (Fig. 2, *c*, *d*). Therefore, all discussed combinations of measurement systems and models practically resulted in a uniform half-space with a resistivity proximal or almost identical to that in the true underlying model. It means that the resistivity patterns can be resolved in practice to quite a high accuracy even in presence

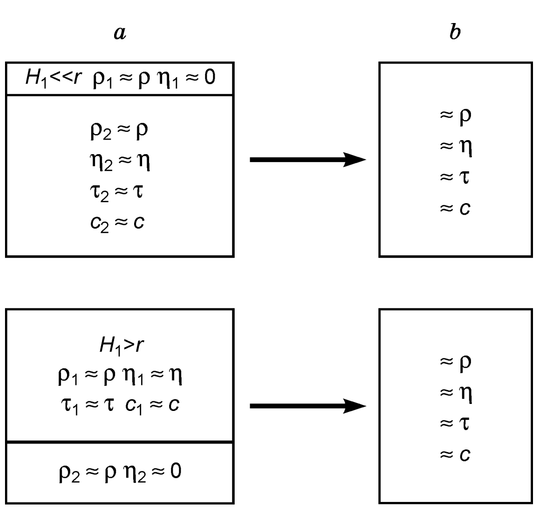

Fig. 3. Two-layer models obtained by inversion without a priori knowledge (*a*) and a model of uniform polarizable half-space they can be reduced to (*b*).

of strong fast-decaying IP effects and in the absence of a priori information.

Looking at Figure 2 it is hard to judge how joint inversion is better than the single one. Model 2 obviously posed the greatest problem (Fig. 2, *b*, *e*, *f*) because of a very low chargeability of 0.02 (Table 1) with its effect comparable to noise. That was the only model in which joint inversion for chargeability and time constant was more in error than single inversion.

The advantage of joint inversion for the models in Table 1 can be summarized as follows. It reduced the thicknesses (by 10 to 100 times) of the upper nonpolarizable layer in models 1, 2, 3 (Fig. 2, *a*) but increased the thickness of the upper polarizable layer in model 5 and, to some extent, also in model 4. Thus the two-layer models approached in their parameters a uniform earth.

The normalized results of the repeated inversion with a priori information are shown in Fig. 4. The main point is that both single and joint inversion gave practically "true" resistivities ρ. In single inversion, the other parameters (η, τ, c) were in a large error. However, joint inversion brought all parameters closer to the initial model: the chargeability η (Fig. 4, *b*), the exponent c (Fig. 4, *d*), and especially the time constant τ (Fig. 4, *c*). It is pertinent to note that joint inversion with minimum a priori knowledge allowed a better fit also for the hardest model 2 unlike the case when the interpreter was unaware of the true model.

Plots in Fig. 5 illustrate how the standard error σ changes in different models. It varied from 2.5 to 30% in the absence of a priori information and from 2.5 to 26% when information became available. In the former case, the mean error σ was 14% for the 50 m × 50 m loop, 4.3% for the 200 m × 50 m loop, and 16% in joint inversion for both loops. In the latter case it improved to $\sigma = 13.6\%$ for the 50 m × 50 m loop, 3.9% for the 200 m × 50 m loop and 12.5% in joint inversion.

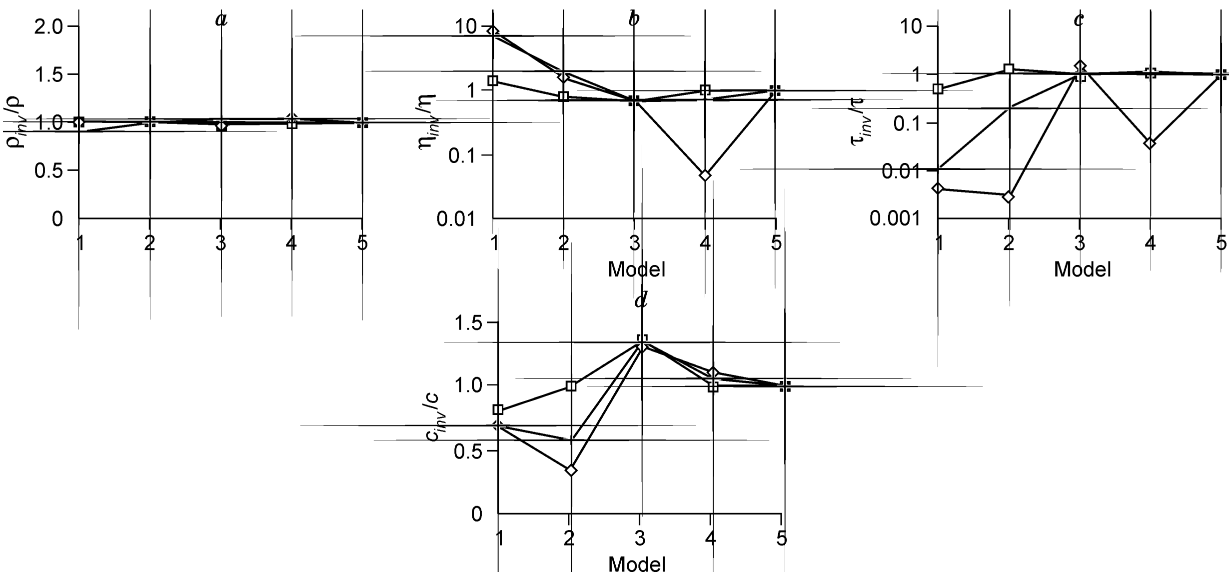

Fig. 4. Parameters obtained by single and joint inversion of transients for different true models (Table 1). The interpreter knew that all initial models corresponded to uniform polarizable conductive half-space. Symbols same as in Fig. 2.

The error estimates and the plots of Fig. 5 allow the following inferences: (i) single inversion of the 200 m × 50 m loop transients is times more accurate than that for the 50 m × 50 m loop and than joint inversion; (ii) models derived from joint inversion are closer to the true models on average but the error σ remains the same as in inversion for the 50 m × 50 m loop; (iii) the availability of a priori information, especially in joint inversion, allows a better fit to the initial models but the resulting error σ is almost the same as in single inversion.

Therefore, the 50 m × 50 m loop data are crucial in inversion of transients measured in a uniform polarizable half-space. This inference is consistent with our earlier conclusion that the IP effect was relatively stronger in data of smaller loops (Kozhevnikov and Artemenko, 2004; Kozhevnikov and Antonov, 2006). Thus, the fit in joint inversion is largely due to the contribution from the 50 m × 50 m loop transients, though error in coincident-loop data is 2.5 times that in central-loop responses.

If chargeability is rather low and it is unknown a priori whether the half-space is polarizable, the 200 m × 50 m loop transients can be interpreted in terms of a nonpolarizable layered earth, whereas data from a small loop cannot be interpreted without invoking IP effects even at moderate chargeability.

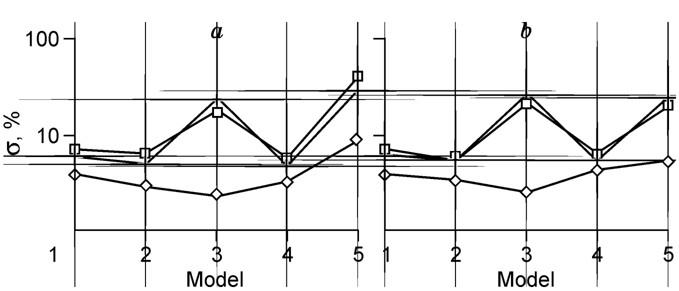

Fig. 5. Relative standard errors of inversion for different initial models, without (*a*) and with (*b*) a priori information. Symbols same as in Fig. 2.

What is the cause of quite a large average error in single (14%) as well as joint (15%) inversion of 50 m × 50 m data? According to the experience we have gained through the reported study, the primary cause is that the smaller-loop transients in a polarizable half-space usually contain a region of monotony break or sign reversal (Fig. 1). In this region, the signal changes very rapidly and its absolute values are vanishing in the vicinity of the sign reversal point. Minor changes in the TEM response within this region, which is the principal carrier of IP message, can cause a relatively large error in inversion. The time delays used in our experiment approached the built-in delays in the available TEM instruments. The sampling intervals are in most cases sufficient to resolve common responses of nonpolarizable conductors but are insufficient for inversion of IP-affected transients. Inversion of the latter, especially in the region of monotony break and/or sign reversal, requires a sampling interval which can allow for the rapidly changing signal.

One might expect to improve the inversion quality by using the absolute rather than relative error in the equation of minimized functional in the region where the fitted transient passes through zero. Note, however, that this approach is poorly practicable because the decaying measured signal becomes 6 or 7 orders of magnitude lower during the time of measurements. The absolute measurement error changes correspondingly, and using it instead of relative error in (1) will strongly reduce the sensitivity of the greatest part of transients to changes in earth's parameters. In some cases we achieved a better inversion quality by closer examination of the problematic near-zero regions in transients and subsequent rejection of worse data from the joint dataset.

The 200 m × 50 m central-loop transients being less strongly affected by fast-decaying IP (see above), transients of large loops are especially important for improving the stability of inversion-derived resistivities, more so that the error is rather small.

Conclusions

The effect of loop configuration on the measured IP-affected transients and, especially, the potentialities of joint inversion of coincident- and central-loop responses of polarizable earth remain poorly studied. We have tried to assess the performance of this inversion using simulation with starting models of a uniform polarizable half-space.

The fitted models, though some of them differed rather strongly from the true ones, provided a good idea of the resistivity pattern, even in single inversion of coincident-loop data and in the absence of a priori information; the availability of a priori information ensured a still better fit. Joint inversion of central-loop and coincident-loop data as a rule brought the model structure and parameters closer to the initial model. When the interpreter was aware of the starting assumptions, joint inversion was of good quality even at a chargeability as low as 0.02.

The rms error of joint inversion depended mainly on the fitting error for smaller-loop transients. It was times the instrumental error and was due to the fact that IP-affected responses contained regions of monotony break or sign reversal where the signal changed too rapidly.

The manuscript profited much from constructive criticism by L.A. Tabarovsky and an anonymous reviewer. The study was supported by grant 07-05-00305 from the Russian Foundation for Basic Research.

References

Kamenetsky, F.M., Sidorov, V.A., Timofeev, V.M., Yakhin, A.M., 1990. TEM processes in conductive polarizable earth, in: Kamenetsky, F.M., Svetov, B.S. (Eds.), Electromagnetic Induction in the Upper Crust [in Russian]. Nauka, Moscow, pp. 14–40.

Kozhevnikov, N.O., Antonov, E.Y., 2006. Fast-decaying IP in frozen unconsolidated rocks and potentialities for its use in permafrost-related TEM studies. Geophysical Prospecting 54, 383–397.

Kozhevnikov, N.O., Antonov, E.Yu., 2007. Fast-decaying IP in unconsolidated frozen ground: A numerical experiment for a uniform polarizable earth. Geofizika, No. 1, 42–50.

Kozhevnikov, N.O, Artemenko, I.V., 2004. Modeling the effect of dielectric relaxation in frozen ground on ungrounded-loop transient responses. Kriosfera Zemli 8 (2), 30–39.

Lee, T., 1981. Transient response of a polarizable ground. Geophysics 46, 1037–1041.

Nelder, J.A., Mead, R., 1965. A simplex method for function minimization. Computer Journal 7, 308–313.

Sidorov, V.A., Yakhin, A.M., 1979. Induced polarization of rocks in TEM soundings. Izv. AN SSSR. Ser. Fizika Zemli, No. 11, 46–52.

Svetov, B.S., Ageev, V.V., Lebedeva, N.A., 1996. Polarizability of rocks and high-resolution resistivity surveys. Geofizika, No. 4, 42–52.

Vanchugov, V.A., Kozhevnikov, N.O., 1998. Methods and results of TEM soundings for the resistivity structure of the Nakyn kimberlite field (Western Yakutia), in: Uchitel, M.S. (Ed.), Geology, Prospecting and Exploration of Mineral Deposits. Collection of Papers [in Russian]. Irkutsk Technological University, Irkutsk, pp. 164–176 (Transactions of Irkutsk Technological University, Issue 22).

Editorial responsibility: M.I. Epov